Title
Molecular Weaving of Covalent Organic Frameworks for Adaptive Guest Inclusion

Journal
Journal of the American Chemical Society, 140(47)

ISSN
0002-7863

Authors
Liu, Yuzhong
Ma, Yanhang
Yang, Jingjing
et al.

Publication Date
2018-11-28

DOI
10.1021/jacs.8b08949

Peer reviewed

Communication

Molecular Weaving of Covalent Organic Frameworks for Adaptive Guest Inclusion

Yuzhong Liu, Yanhang Ma, Jingjing Yang, Christian S. Diercks, Nobumichi Tamura, Fangying Jin, and Omar M. Yaghi

J. Am. Chem. Soc., **Just Accepted Manuscript** • DOI: 10.1021/jacs.8b08949 • Publication Date (Web): 01 Oct 2018

Molecular Weaving of Covalent Organic Frameworks for Adaptive Guest Inclusion

Yuzhong Liu,[†] Yanhang Ma,[‡] Jingjing Yang,[†] Christian S. Diercks,[†] Nobumichi Tamura,[§] Fangying Jin,[†] Omar M. Yaghi[†,*]

[†]Department of Chemistry, University of California-Berkeley, Materials Sciences Division, Lawrence Berkeley National Laboratory, Kavli Energy NanoSciences Institute, Berkeley, California 94720, USA.
[‡]School of Physical Science and Technology, Shanghai Tech University, Shanghai 201210, China.
[§]Advanced Light Source, Lawrence Berkeley National Laboratory, Berkeley, California 94720, United States.

Supporting Information Placeholder

ABSTRACT: The synthesis of new isoreticular non-interpenetrated woven frameworks, COF-506-Cu and COF-506, was achieved by linking aldehyde functionalized copper(I) bisphenanthroline complexes with benzidine linkers in the presence of a bulky anion, diphenylphosphinoate ($PO_2Ph_2^-$). The structures of the frameworks were determined by a combination of powder X-ray diffraction and electron microscopy techniques. Guest-accessibility of the internal surface of the two frameworks, as well as of the related two-fold interpenetrated woven COF-505 was examined by vapor and dye inclusion studies. The demetalated form of COF-506 was found to take up guest molecules that exceed the size of the framework's pores thus giving credence to the notion of a novel mode of dynamic motion of solids, termed 'adaptive inclusion'.

INTRODUCTION

Relative to dynamics observed in discrete molecules, extended solids are commonly perceived as being non-dynamic. With the advent of reticular chemistry, it has become possible to introduce motions into solids by using flexible building blocks[1–3] and dangling switchable[4–6] or mechanically interlocked units[7,8] into the pores (Scheme 1a through c). In this report, we introduce a fourth scenario made possible by the discovery of woven extended structures, where threads of covalently bonded molecules are interlaced at regular intervals to form two- and three-dimensional (2D and 3D) frameworks.[9–12] The fact that the interactions between the threads (mechanical) are much weaker relative to those within the threads (covalent) allows collective large-amplitude movements between them. Openness within such constructs facilitates these movements, while the interlacing prevents unzipping and ensures the fidelity of the overall system. These properties, especially the ease with which the threads can move with respect to each other, are ideally suited for woven frameworks to adapt to incoming guests of various shapes, thus giving rise to 'adaptive dynamics' (Scheme 1d). In biological systems, adaptive binding is commonly credited for combining selectivity with maximizing substrate-host interactions to affect highly specific functions. Adaptive dynamics being reliant on mechanical interlacing of threads as described in here forgoes the need to stretch and bend bonds throughout an extended structure to achieve collective motion.

The first generation of woven COFs were found to be dense structures with little internal guest-accessible void space.[9,10] This posed an intrinsic limitation to the COF's dynamic behavior as the openness of woven constructs dictates the magnitude of their dynamic motion. Here, we report the synthesis and crystal structures of a new isoreticular woven COF-506-Cu (Scheme 2, -Cu indicates the metalated form of the woven COF), and porosity studies done on COF-506-Cu, COF-506 (demetalated), as well as the previously reported COF-505-Cu as a reference point to evaluate the effects of pore size and degrees of interpenetration on the dynamics of these frameworks. The crystal structure COF-506-Cu was determined by a combined transmission electron microscopy, 3D electron diffraction tomography, and powder X-ray diffraction approach. Vapor and dye inclusion in these structures is studied to probe the porosity and adaptive dynamics of the investigated frameworks.

Scheme 1. Different Modes of Dynamics in Solids. (a) Flexible Constituents Yield Frameworks that Distort in Response to External Stimuli. (b) Mechanically Interlocked Molecules Appended onto the Struts Move within the Constraints Imposed by the Framework. (c) Switchable Units Dangling in the Pores Respond to External Stimuli by Conformational Changes, and (d) Adaptive Inclusion of Guests in Woven Frameworks where Large Degrees of Freedom of the Threads Allow for Adaptive Inclusion of Guests.

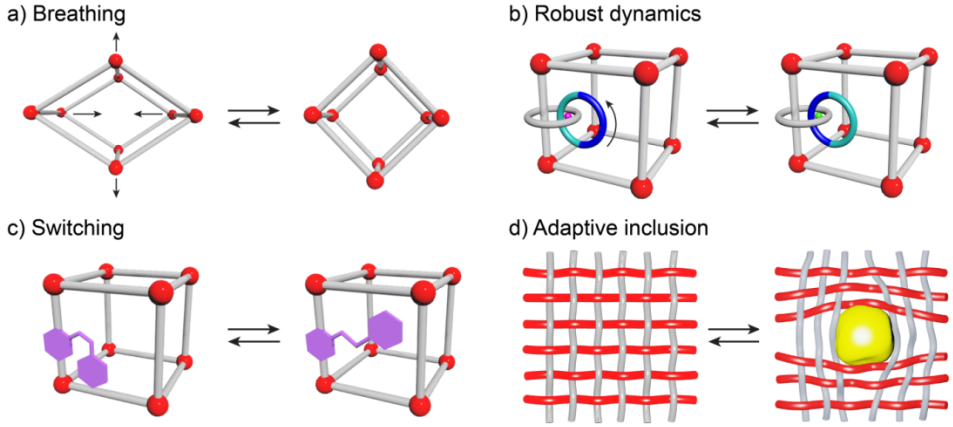

RESULTS AND DISCUSSION

Designed synthesis and characterization of COF-506-Cu. We previously reported the design and synthesis of the first woven framework, COF-505-Cu, using an aldehyde-functionalized $Cu(PDB)_2BF_4$ complex as the tetrahedral building block, which was reticulated with a linear ditopic benzidine (BZ) linker to yield a 2-fold interpenetrated 3D framework with an underlying **dia** topology (Scheme 2a). **dia** nets are self-dual and as such prone to self-interpenetration.[13] In the case of COF-505-Cu, this limited the available internal space and restricted the dynamic motion of the threads. To avoid interpenetration during framework formation and maximize the guest accessible void space a bulky anion ($PO_2Ph_2^-$, diphenylphosphinoate) is used to occupy the internal voids in COF-506-Cu. The anions are then post-synthetically exchanged with BF_4^- to obtain the non-interpenentrated structure COF-506-Cu (Scheme 2b).

COF-506-Cu was synthesized under solvothermal conditions (Section S2). Completion of the reaction was confirmed by fourier-transform infrared spectroscopy (FT-IR) where the emergence of a peak at 1623 cm^{-1} (Figures S2 to S4, 1622 cm^{-1} for COF-505-Cu) was assigned to the characteristic C=N stretching mode of formed imine bonds. Furthermore, the post-synthetic anion exchange of COF-506-Cu was confirmed by the presence of a prominent band at 1057 cm^{-1}, assigned to the asymmetric stretching mode of BF_4^-.[14] Furthermore, the ^{1}H-NMR spectrum of acid-digested COF shows an equimolar ratio of the starting materials (PDB *vs*. BZ) confirming completion of the COF-forming imine condensation reaction (Section S5).

Scheme 2. Synthetic Scheme for the Formation of COF-506-Cu with Underlying dia Topology, as well as COF-505-Cu, its Interpenetrated Analog.

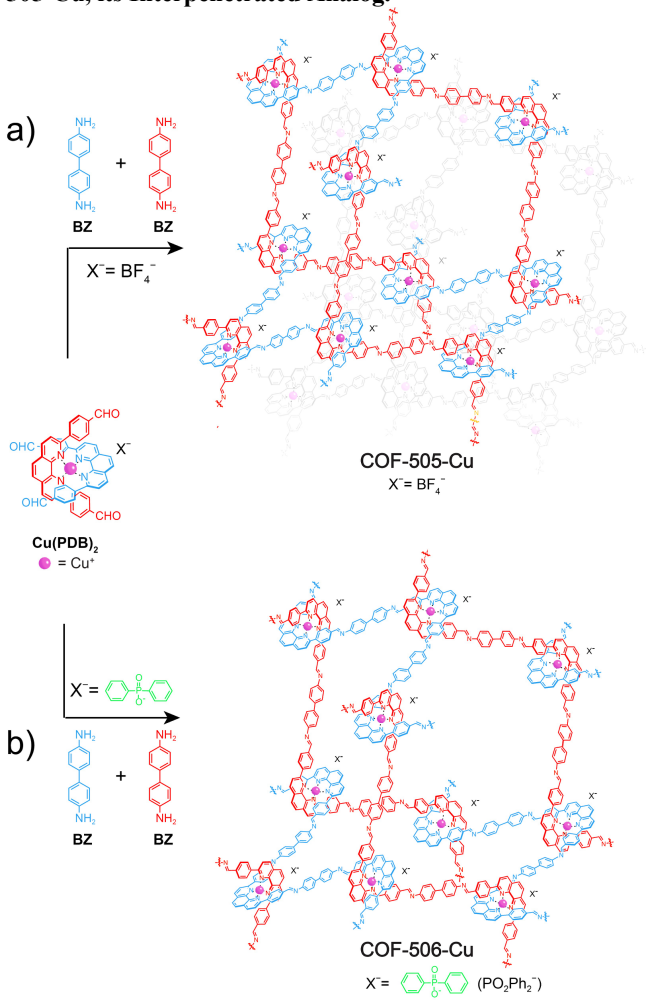

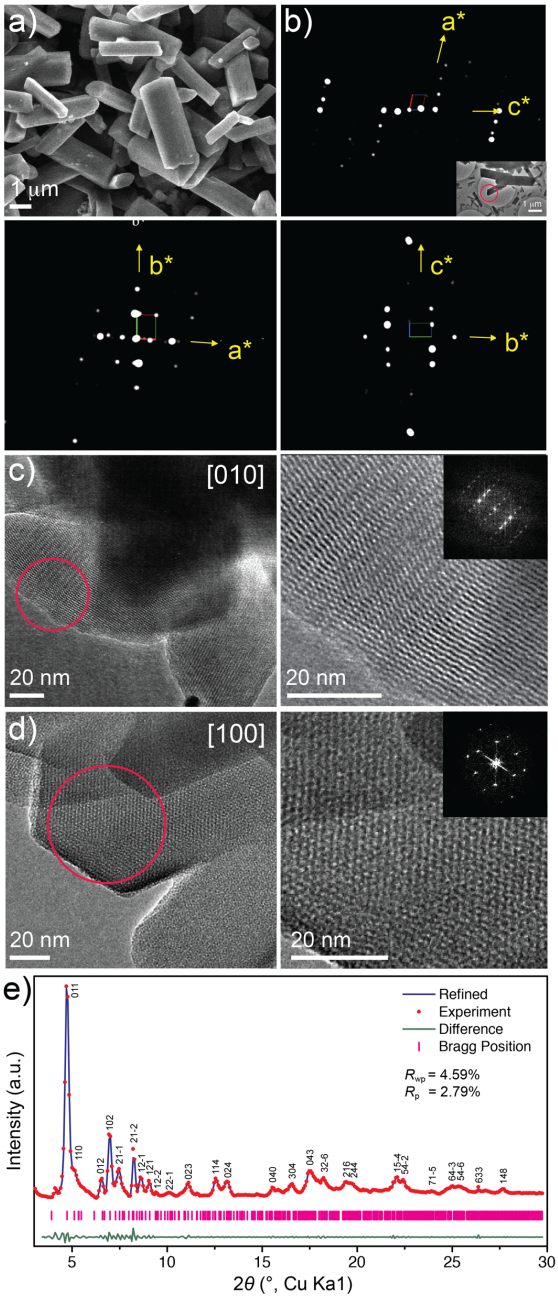

Figure 1. Electron microscopy and X-ray diffraction studies of COF-506-Cu. (**a**) SEM shows rod-shaped single crystals of COF-506-Cu. (**b**) 2D projection of the reconstructed reciprocal lattice of COF-506-Cu obtained from 3D-EDT data. Inset, TEM image of a single crystal used for 3D-EDT. (**c**) and (**d**) HRTEM images of COF-506-Cu taken with [010] and [100] incidence and magnified views of the circled areas with FFT (inset) are in good agreement with the experimental measurements in (**b**). (**e**) Indexed PXRD pattern of activated COF-506-Cu (red, $PO_2Ph_2^-$ counter anions) and Pawley refinement (blue) against the modeled structure. The pattern does not change upon anion exchange to BF_4^-. The difference plot and calculated Bragg positions are highlighted in green and pink, respectively.

Structure determination of COF-506-Cu. The morphology and purity of the as-synthesized material were studied by scanning electron microscopy (SEM) where a single phase of rod-shaped crystals of several micrometers in length (Figure 1a) were observed. One single crystal (Figure 1b inset) was then chosen for 3D electron diffraction tomography studies (3D-EDT).[15] A data set was collected (Figure 1b) by combining specimen tilt and electron-beam tilt in the range of –30.2° to +41.2° with a beam-tilt step of 0.2°. The 3D reciprocal lattice of COF-506-Cu was constructed and identified as a monoclinic Bravais lattice with unit cell parameters of a = 27.7 Å, b = 21.9 Å, c = 33.8 Å, β = 104°, and V = 19895 Å^3, which were further refined to be a = 27.0 Å, b = 23.1 Å, c = 34.6 Å, β = 108°, and V = 20533 Å^3 by Pawley refinement against the experimental PXRD pattern. High-resolution TEM (HRTEM) images viewed from the [010] and [001] directions show ordered lattice fringes and the resultant fast Fourier transform (FFT) matches well with the experimental dataset of the 3D-EDT (Figure 1c and d). According to these parameters, a structure model of COF-506 was constructed in the monoclinic space group *Pc* (Section S7).[15] The calculated PXRD pattern of the modeled structure was found to be in good agreement with the experimental pattern of activated COF-506-Cu (Figure 1e).

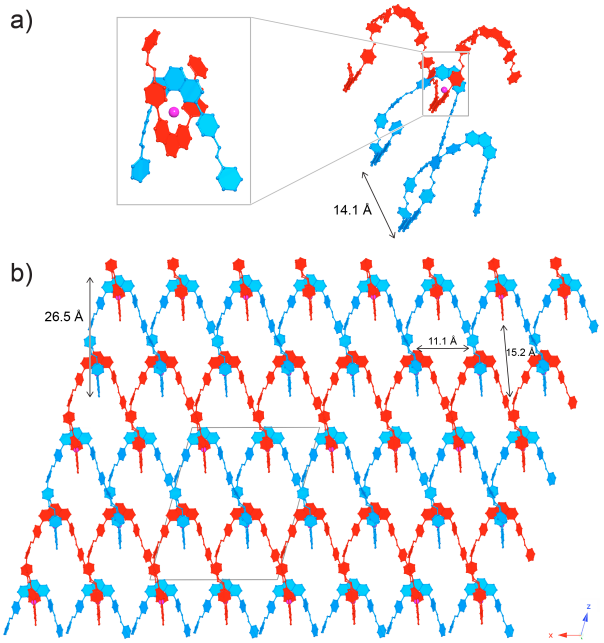

Figure 2. Crystal structure of woven COF-506-Cu. (**a**) COF-506-Cu consists of 1D helices with a pitch of 14.1 Å. (**b**) Helices highlighted in blue and red propagate in the [110] and [-110] direction, respectively with copper(I) ions (pink) serving as points of registry. Neighboring blue and red helices are woven to form the overall framework viewed along the *b* axis. All hydrogen atoms are omitted for clarity.

In the crystal structure of woven COF-506-Cu, tetratopic $Cu(PDB)_2$ constituents are linked by linear ditopic BZ to yield a framework with underlying **dia** topology (Figure 2). COF-506-Cu consists of chemically identical polyimine helices with a pitch of 14.1 Å that propagate along the [110]

and [-110] directions (highlighted in blue and red) to construct a 3D pore system with the largest channels of 11.1 Å × 15.2 Å running along the crystallographic *b* direction.

THF vapor adsorption and dye inclusion studies. To test whether the internal void space of the woven COF-506-Cu and the reported COF-505-Cu are guest-accessible, the structures were examined by THF vapor adsorption (Section S8). COF-505-Cu shows a negligible uptake of THF, which is attributed to the relatively small pores that are occupied by solvated BF_4^- anions. In contrast, COF-506-Cu exhibits an isotherm with a major uptake at low partial pressure indicative of a microporous material. The first step in the isotherm is reached at P/P_0 = 0.2 with 39.6 cm^3g^{-1} and the maximum uptake reached 56.6 cm^3g^{-1} at P/P_0 = 0.98.

Furthermore, inclusion studies with anionic fluorescent dyes[17–19] of increasing sizes [methyl orange (MO) < hydroxynaphthol blue disodium salt (HN) < methyl blue (MB)] were employed to evaluate the dimensions of the guest-accessible voids. 5 mg of activated COF were immersed in a 100 ppm methanol solution containing the guest compound to be included. The amount of molecules in the supernatant was measured using ultraviolet-visible (UV-Vis) spectrophotometry, and the characteristic absorbance at 432 nm (MO), 540 nm (HN), or 606 nm (MB) was monitored over a period of 3 hours. Owing to the positively charged framework backbone, the uptake of the anionic dyes can be attributed to a combination of adsorption and anion exchange. Nevertheless, it provides insight into the accessible pore dimensions of the frameworks. The results are plotted in Figure 3, and clearly show a continuous decrease of the amount of MO in the supernatant in the presence of COF-506-Cu, while only a negligible amount of inclusion was observed for COF-505-Cu (Section S9). As the size of the dye increases, a significant amount of HN was only adsorbed by COF-506-Cu. Finally, in the case of MB, both frameworks did not display any major uptake. In summary, the pore dimensions increase significantly from COF-505-Cu to COF-506-Cu, in good agreement with their crystal structures.

Dye adsorption in COF-506. The copper(I) ions in COF-506-Cu were removed to probe for resultant dynamic behavior. This was affected by heating in a 1M KCN methanol solution at 75 °C yielding COF-506. Inductively coupled plasma atomic emission spectroscopy analysis revealed that 99% of the copper ions were removed. Under the same conditions, COF-505-Cu could not be demetalated due to limited accessibility of its internal surface. Upon demetalation, the drastically decreased crystallinity of COF-506 and the disappearance of lattice fringes in the TEM micrographs (Figure 3d) indicate spatial rearrangement of the structure and loss of long-range periodicity. In contrast, the morphology of the crystals remained unaffected which is attributed to the fact that the overall connectivity of the structure is retained. This is corroborated by the fact that the chemical integrity of the structure was maintained: The FT-IR imine stretching vibration at 1623 cm^{-1} in COF-506 is identical to the one of its metalated progenitor.

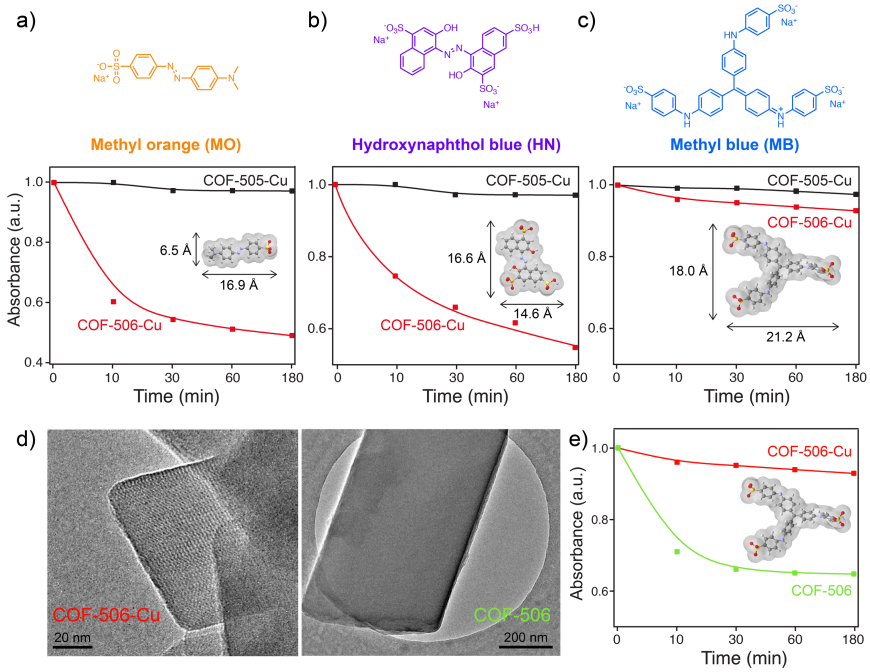

Figure 3. Inclusion studies of COF-505-Cu (black), COF-506-Cu (red), and COF-506 (green) with anionic dye molecules: (**a**) Methyl orange (MO), (**b**) hyroxynaphthol blue (NH), and (**c**) methyl blue (MB). (**d**) TEM images of COF-506-Cu and COF-506. Upon demetalation, the lattice fringes indicative of the framework's crystalline nature disappeared while the morphology of the single crystal was retained. (**e**) MB uptake of COF-506 compared to COF-506-Cu.

The inclusion of MB dye in COF-506 shows a major uptake, 11.6-fold higher than that of its metalated analog (Figure 3e). Upon demetalation, the absence of copper(I) ions allows for spatial deviation of the threads to move about the points of registry and to accommodate the inclusion of dye molecules that cannot fit within its metalated form. It should be noted that the higher uptake cannot be rationalized by the absence of counterions in the pores since these would be exchanged by the negatively-charged dye. As such, anisotropic structural rearrangements are necessary to open up the framework — the structure adapts to accommodate the guest molecule.

ASSOCIATED CONTENT

The Supporting Information contains synthetic protocols, powder x-ray diffraction analysis, structural modelling, and details on vapor, as well as dye inclusion studies. This material is available free of charge via the internet at http://pubs.acs.org.

AUTHOR INFORMATION

Corresponding Author

*yaghi@berkeley.edu

Notes

The authors declare no competing financial interests.

ACKNOWLEDGMENT

The crystal structure of $Cu(PDB)_2PO_2Ph_2$ is available from the Cambridge Crystallographic Data Centre under the reference number CCDC-1870357. Financial support for COF research in the O.M.Y. laboratory was provided by KACST through the UC Berkeley-KACST Joint Center of Excellence for Nanomaterials for Clean Energy Applications, King Abdulaziz City for Science and Technology. Y.L. was supported by the Philomathia Graduate Student Fellowship in the Environmental Sciences. C.S.D. would like to acknowledge the Kavli foundation for funding through a Kavli ENSI graduate student fellowship. The Advanced Light Source is supported by the Director, Office of Science, Office of Basic Energy Sciences, of the U.S. Department of Energy under Contract No. DE-AC02-05CH11231. The authors acknowledge Dr. Zheng Liu for high resolution transmission electron microscopy data requisition, Xiaokun Pei and Dr. Eugene A. Kapustin for help with X-ray diffraction.

REFERENCES

(1) Serre, C.; Millange, F.; Thouvenot, C.; Noguès, M.; Marsolier, G.; Louër, D.; Férey, G. *J. Am. Chem. Soc.* **2002**, *124*, 13519–13526.
(2) Férey, G.; Serre, C. *Chem. Soc. Rev.* **2009**, *38*, 1380–1399.
(3) Krause, S.; Bon, V.; Senkovska, I.; Stoeck, U.; Wallacher, D.; Többens, D. M.; Zander, S.; Pillai, R. S.; Maurin, G.; Coudert, F.-X.; Kasel, S. *Nature* **2016**, *532*, 348–352.
(4) Brown, J. W.; Henderson, B. L.; Kiesz, M. D.; Whalley, A. C.; Morris, W.; Grunder, S.; Deng, H.; Furukawa, H.; Zink, J. I.; Stoddart, J. F.; Yaghi, O. M. *Chem. Sci.* **2013**, *4*, 2858–2864.
(5) Schneemann, A.; Bon, V.; Schwedler, I.; Senkovska, I.; Kaskel, S.; Fischer, R. A. *Chem. Soc. Rev.* **2014**, *43*, 6062–6096.
(6) Horike, S.; Shimomura, S.; Kitagawa, S. *Nat. Chem.* **2009**, *1*, 695–704.
(7) Zhao, Y. L.; Liu, L.; Zhang, W.; Sue, C. H.; Li, Q.; Miljanić, O. Š.; Yaghi, O. M.; Stoddart, J. F. *Chem. - A Eur. J.* **2009**, *15*, 13356–13380.
(8) Deng, H.; Olson, M. A.; Stoddart, J. F.; Yaghi, O. M. *Nat. Chem.* **2010**, *2*, 439–443.
(9) Liu, Y.; Ma, Y.; Zhao, Y.; Sun, X.; Gandara, F.; Furukawa, H.; Liu, Z.; Zhu, H.; Zhu, C.; Suenaga, K.; Oleynikov, P.; Alshammari, A. S.; Zhang, X.; erasaki, O.; Yaghi, O. M. *Science* **2016**, *351*, 365–369.
(10) Zhao, Y.; Guo, L.; Gándara, F.; Ma, Y.; Liu, Z.; Zhu, C.; Lyu, H.; Trickett, C. A.; Kapustin, E. A.; Terasaki, O.; Yaghi, O. M. *J. Am. Chem. Soc.* **2017**, *139*, 13166–13172.
(11) Liu, Y.; O'Keeffe, M.; Treacy, M. M. J.; Yaghi, O. M. *Chem. Soc. Rev.* **2018**, *47*, 4642-4664.
(12) Liu, Y.; Yaghi, O.M. *Bull. Jpn. Coord. Chem.* 2018, *71*, 12-17.
(13) Friedrichs, O. D.; O'Keeffe, M.; Yaghi, O. M. *Solid State Sci.* **2003**, *5*, 73–78.
(14) Heimer, N. E.; Del Sesto, R. E.; Meng, Z.; Wilkes, J. S.; Carper, W. R. *J. Mol. Liq.* **2006**, *124*, 84–95.
(15) Gemmi, M.; Oleynikov, P. *Zeitschrift fur Krist.* **2013**, *228*, 51–58.
(16) Dassault Systèmes BIOVIA, Materials Studio 8.0, San Diego: Dassault Systèmes (2014).
(17) Ning, G. H.; Chen, Z.; Gao, Q.; Tang, W.; Chen, Z.; Liu, C.; Tian, B.; Li, X.; Loh, K. P. *J. Am. Chem. Soc.* **2017**, *139*, 8897–8904.
(18) Fang, Q.; Zhuang, Z.; Gu, S.; Kaspar, R. B.; Zheng, J.; Wang, J.; Qiu, S.; Yan, Y. *Nat. Commun.* **2014**, *5*, 4503.
(19) Haque, E.; Jun, J. W.; Jhung, S. H. *J. Hazard. Mater.* **2011**, *185*, 507–511.

Table of Contents Figure